

## Slow positrons in metal single crystals. I. Positronium formation at Ag(100), Ag(111), and Cu(111) surfaces

K. G. Lynn and D. O. Welch

Brookhaven National Laboratory, Upton, New York 11973

(Received 13 July 1979)

Monoenergetic positrons, with an incident energy of 0–5 keV, were focused onto Ag(100), Ag(111), and Cu(111) surfaces with submonolayer contamination, and positronium formation was studied as a function of sample temperature from 300 to 1200 K. The data were fitted with a simple positron diffusion model including surface and vacancy trapping, assuming that positronium is formed only at the surface. The formation of part of the positronium fraction is found to be a temperature-activated process which is identified as detrapping from a surface state, and an estimate of the binding energy in this trap is deduced. The diffusion length is found to be only slightly temperature dependent between room temperature and the onset of vacancy trapping. At the higher sample temperatures positron trapping at thermally generated vacancies is observed by the decrease in the positron diffusion length at the higher incident voltages. A vacancy formation energy is extracted from the data and is generally found to be lower than the values obtained from bulk measurements.

### I. INTRODUCTION

The experiments of Canter *et al.*,<sup>1</sup> Mills,<sup>2</sup> and Lynn<sup>3</sup> have shown that positronium (Ps) forms with high efficiency when slow positrons impinge on metallic surfaces. Since it is believed that the electron density within a metal is too high to permit the formation of Ps,<sup>4</sup> and since Ps has not been positively observed to form in the presence of vacancies or even voids produced by neutron irradiation,<sup>5</sup> it is reasonable to assume that the observed Ps is formed at or near the metal surface, rather than internally.

The experiments of Canter *et al.*<sup>1</sup> were performed in a vacuum where the surface condition of the sample was unknown. Thus the question of the role of surface oxides or other contaminants in the formation of Ps was left unanswered. However Mills,<sup>2</sup> utilizing an ultrahigh-vacuum system, reported that Ps formation is the dominant process for slow positrons incident on Al, Ge, and Si with submonolayer surface contamination and attributed the observed Ps to thermalized positrons that diffuse back to the surface and form Ps in the surface region. The efficiency of Ps formation was observed to be dependent on temperature and upon the energy of the implanted positron.<sup>1–3</sup> Recently Lynn<sup>3,6</sup> and Mills<sup>7</sup> have identified the increase of the Ps fraction with temperature as a thermally activated process from the surface state. Mills<sup>7</sup> also used these extracted activation energies in a Born-Haber cycle which produced positron surface binding energies in reasonable agreement with previous theoretical predictions.<sup>8</sup>

In this paper, we report a study of the formation of positronium as a function of sample temperature

(300–1200 K) and the energy (0–5 keV) of positrons incident on Ag(100), Ag(111), and Cu(111) surfaces with submonolayer contamination. The results are analyzed in the context of a simple diffusion model which includes the effects of positron trapping by the surface and by thermally generated vacancies. Surface trap depths and vacancy formation energies are extracted from the data.

### II. EXPERIMENTAL APPARATUS AND METHOD

The slow positron beam is similar in design to that of Canter *et al.*,<sup>1</sup> but has been modified to ultrahigh-vacuum conditions. The beam consists of a series of split solenoids with a 45° bend near the source end. The surface and source chambers can be isolated by an all metal valve; therefore either end of the beam line can be brought to atmospheric pressure independently. The entire beam line is stainless steel and is bakeable to 200°C.

Annealed Cu is used for the positron moderator.<sup>9</sup> This moderator can be ion sputtered and indirectly heated by electron bombardment to 1000°C. The energy resolution of the emitted positrons is approximately 300 meV at 20 volts incident positron energy. We confirm the Mills<sup>9</sup> result that this Cu convertor is superior to the more standard smoked MgO on Au or Pt.<sup>10</sup> In other words the convertor has a high slow positron efficiency and good long-term stability in the slow positron yield.

After the beam is accelerated away from the moderator it can be collimated in both dimensions perpendicular to the beam axis. The beam diameter

is approximately 0.64 cm. A channeltron can be moved into the beam to check the positron current before it proceeds through a ten-stage electrostatic accelerator. Beyond the accelerator a 97% transmission Cu grid can be inserted before the sample. (This grid is used mainly in positron work function measurements.)

The sample target is mounted on a Ta foil which is spot welded to Ta posts. Two thermocouples behind or on the sample are used to measure the temperature. When the sample temperature was reduced we found that systematic errors could be produced from thermal lag of the crystal, especially at the lower temperatures. All insulators are either protected or removed from the target area to reduce electric fields associated with charging. The sample can be positioned for ion sputtering, low-energy electron diffraction (LEED), and retarding field Auger electron spectroscopy (AES). The LEED and AES systems utilized standard Varian four-grid LEED optics. A glancing incidence electron gun as well as the integral normal incidence gun are available for sample characterization by AES. The vacuum was monitored throughout the experimental runs and varied with the sample temperature but was typically between  $5 \times 10^{-11}$  and  $5 \times 10^{-10}$  Torr.

If the target was directly heated all of the electronics were gated off when current was flowing through the sample. Indirect heating with electrons was also used for lower temperatures. A full description of the apparatus will be published elsewhere.<sup>11</sup>

The Ag and Cu single-crystal samples, approximately 2.5 cm in diameter, were oriented to  $1^\circ$  using x-rays. Both samples were annealed before insertion into the vacuum system and measured again with x-rays to observe if recrystallization had occurred. The Cu sample was also baked in  $H_2$  gas for 1 week at  $650^\circ C$  to remove sulfur from the bulk. At high temperatures the sulfur impurities segregate at the surface and affect the Ps fraction as well as the reemission of positrons from the surface.<sup>9</sup> Before and after each run a retarding field Auger and LEED measurement was performed. We found approximately 0.01 monolayer of P and C on the Ag and 0.10 monolayer of S on the Cu sample after the experimental run calculated in the manner outlined in Physical Electronic Industries Handbook of Auger Electron Spectroscopy. We did observe a small hysteresis in the positronium fraction for some runs which we associated with these impurities. For example, oxygen on Ag (Ref. 12) can produce a negative positron work function,  $\Phi_p$  (favorable for reemission of a free positron into the vacuum).

When Ps forms, the statistical weight will produce three times as much *o*-Ps ( $^3S_1$ ) as *p*-Ps ( $^1S_0$ ). The  $^1S_0$  state primarily decays into two photons, with the energy of each photon being very close to  $m_0c^2$  (511 keV). The  $^3S_1$  (assuming no pickoff annihilation)

decays primarily into three photons with a continuous energy distribution for each of the photons ranging from approximately 0 to  $m_0c^2$ .<sup>13</sup> By measuring the change in the ratio of the photopeak to the total spectrum, one can detect the formation of Ps.

In these experiments either a  $7.5 \times 7.5$  cm<sup>2</sup> NaI(Tl) or a Ge(Li) detector was mounted directly behind the target. The NaI(Tl) was coupled to an approximately 36-in. light pipe which removed the photomultiplier tube from the magnetic field produced by the split solenoid coils. Water or air cooling was used to keep the detector at room temperature. Three single-channel analyzers (SCA) were used to measure the counting rates in three regions of the NaI(Tl) or Ge(Li) energy spectrum. The voltage windows on the SCA's, corresponded to  $80 \leq E \leq 570$  keV,  $450 \leq E \leq 570$  keV, and  $360 \leq E \leq 450$  keV which represented the total energy range ( $T_f$ ), photopeak ( $P_f$ ), and valley ( $V_f$ ) for the NaI detector, respectively. Similar energy windows were set for the Ge(Li) detector, except for the photopeak ( $P_f$ ) which was narrower owing to the improved detector resolution. The full-width-at-half-maximum (FWHM) for a 514-keV  $\gamma$ -ray in the Ge(Li) detector was 1.35 keV, whereas the NaI(Tl) detector produced a FWHM as poor as 80 keV, owing to the light pipe configuration. One could just as easily choose some other restricted energy range and the equations below would be equally valid, although the statistical uncertainty would be different. For example in choosing the narrow region in the valley of the spectrum one gains sensitivity but loses statistical accuracy. A multichannel analyzer was also used to monitor the energy spectrum during an experimental run.

With the NaI(Tl) detector we observed a shift toward lower energies in the peak when large amounts of Ps were produced, owing to the convolution of the detector resolution with the asymmetric energy distribution of the emitted  $\gamma$ -rays from the  $^3S_1$ .<sup>14</sup> With a computer simulation study<sup>15</sup> we found that the peak shift produced by the convolution of the detector resolution with the  $^3S_1$   $\gamma$ -rays did not show any significant systematic error in the extracted Ps fraction, for either detector resolution. However, this systematic effect should be removed when measuring the red shift with a Ge(Li) detector produced from the  $^1S_0$  Ps emitted from the target surface. If not taken into account this systematic error will produce an error in the emitted Ps energy distribution.

### III. EXPERIMENTAL RESULTS

To determine the fraction  $F$  of Ps atoms produced at the surface of the sample we will derive an expression which follows the work of Marder *et al.*<sup>16</sup> and has been used by Mills<sup>2</sup> and Lynn.<sup>3</sup> With the small

magnetic field employed in these experiments ( $\sim 70$  G), the effect of magnetically quenching the  $M=0$  state of  $o$ -Ps is very small.<sup>16</sup> The  $M=0$  state of the  $p$ -Ps will similarly have an admixture of the  $o$ -Ps state, but since the annihilation rates of these two states are so different the  $p$ -Ps will decay predominantly by two-photon annihilation.<sup>16</sup>

The total ( $T_f$ ) and peak ( $P_f$ ) regions have been chosen arbitrarily and are represented by the following equations:

$$P_f = N_a(1-F)g_p + FN_o g_o + FN_p g_p, \quad (1a)$$

$$T_f = N_a(1-F)h_p + FN_o h_o + FN_p h_p, \quad (1b)$$

where the subscript  $F$  refers to the fraction of Ps formed in the target region. The quantities  $N_a$ ,  $N_p$ , and  $N_o$  are the number of counts per unit time for the free-positron-electron annihilations in the metal or surface trap, the  $p$ -Ps annihilations, and  $o$ -Ps annihilations, respectively. The quantities  $g_o$  and  $h_o$  are, respectively, the average probability that a  $\gamma$ -photon from the  $o$ -Ps decay will be counted in the peak or in the total energy spectrum. The average probability that an annihilation  $\gamma$ -ray from a  $p$ -Ps decay will be counted in the peak region or in the total part of the energy spectrum is  $g_p$  and  $h_p$ , respectively. Free-positron-electron annihilations will be assigned the same average probability as that for  $p$ -Ps. These factors depend upon the spatial distribution of annihilation events, resolution, and efficiency of the detector system, scattering events which cause degradation of the annihilation photons and the solid angle subtended by the  $\gamma$ -ray detector.

These equations implicitly assume that the same probability factors are used in all cases. One would expect a small difference between  $F=0$  and 1 as the  $o$ -Ps will drift away from the target and change the spatial distribution of the annihilations. Now by forming the ratio [ $R_f = (T_f - P_f)/P_f$ ], thereby eliminating variations in the beam current, between 0 and 100% fraction, substituting Eqs. (1a) and (1b) in the above equation and solving for  $F$  we find

$$F = \left[ 1 + \frac{P_1}{P_0} \left( \frac{R_1 - R_f}{R_f - R_0} \right) \right]^{-1}, \quad (2)$$

where the subscripts 0 and 1 correspond to Eqs. (1) for 0% and 100% Ps formation. To obtain  $R_0$ , the curves of  $T_f$  and  $P_f$  are extrapolated to high-incident positron energy ( $>20$  keV) from either the low- or high-temperature data yielding the limiting values  $T_0$  and  $P_0$  corresponding to 0% Ps production. The experimental values for each sample were deduced separately. Uncertainties in the extrapolation process for  $R_0$  and  $P_0$  contribute a  $\pm 0.10$  systematic error in the positronium fraction. The quoted errors in the positronium fraction are approximated by the variations in the extrapolation process for  $P_0$ ,  $P_1$ ,  $R_0$ , and

TABLE I. The parameters  $F_0$  and  $E_0$  which were extracted from the fits to Eq. (5). The values of  $R_0$ ,  $R_1$ , and  $P_1/P_0$  used in Eq. (2) are also given. The values in parentheses are the error bars.

$R_{S0}=2.63$ Temp. ( $^{\circ}\text{C}$ )	Ag(100) valley	
	$R_{S1}=1.79$ $F_0$	$V_{S1}/V_{S0}=1.23$ $E_0$
900.0	1.349(0.117)	1809.2(310.01)
850.0	1.290(0.100)	2180.5(350.99)
800.0	1.193(0.041)	2804.1(220.40)
750.0	1.149(0.051)	2999.6(312.44)
700.0	1.130(0.056)	3031.8(353.84)
650.0	1.011(0.044)	3917.5(485.18)
600.0	0.935(0.030)	4114.9(387.52)
550.0	0.854(0.030)	4185.5(435.01)
500.0	0.808(0.028)	4057.9(399.51)
450.0	0.687(0.024)	4114.5(424.44)
400.0	0.572(0.021)	4191.4(453.08)
350.0	0.474(0.015)	4662.3(468.09)
300.0	0.477(0.012)	5731.1(511.29)
250.0	0.411(0.017)	5687.5(729.03)
200.0	0.410(0.007)	6591.4(434.41)
100.0	0.399(0.015)	4473.5(500.24)
$R_0=1.75$ Temp. ( $^{\circ}\text{C}$ )	Ag(111) peak	
	$R_1=3.06$ $F_0$	$P_1/P_0=0.687$ $E_0$
800.0	1.230(0.060)	2705.1(312.21)
750.0	1.187(0.048)	3025.6(301.85)
700.0	1.129(0.038)	3379.4(292.94)
600.0	0.969(0.024)	4257.2(309.12)
550.0	0.871(0.022)	4594.1(342.93)
500.0	0.759(0.021)	4857.1(421.30)
450.0	0.636(0.019)	5191.9(503.00)
400.0	0.539(0.011)	5052.1(331.47)
350.0	0.468(0.013)	4934.3(434.04)
300.0	0.426(0.013)	4867.4(462.03)
250.0	0.391(0.006)	5375.4(268.65)
200.0	0.373(0.014)	5416.7(648.11)
150.0	0.359(0.007)	5368.9(345.32)
100.0	0.345(0.013)	6182.5(825.74)
$R_0=1.77$ Temp. ( $^{\circ}\text{C}$ )	Cu(111) peak	
	$R_1=3.02$ $F_0$	$P_1/P_0=0.679$ $E_0$
835.0	1.181(0.040)	3856.3(356.40)
800.0	1.129(0.032)	4170.1(333.51)
750.0	1.053(0.033)	4617.1(428.86)
700.0	0.928(0.017)	5327.3(322.69)
650.0	0.853(0.022)	5498.9(458.12)
550.0	0.697(0.022)	6193.2(672.17)
500.0	0.665(0.015)	5930.5(467.81)
450.0	0.610(0.016)	6911.3(669.34)
400.0	0.601(0.012)	6786.0(514.13)
350.0	0.589(0.010)	7261.7(457.64)
300.0	0.593(0.010)	6763.9(435.66)
250.0	0.564(0.008)	8095.4(461.27)
200.0	0.563(0.010)	7701.0(552.24)
150.0	0.556(0.011)	7498.1(575.69)
100.0	0.534(0.004)	7991.8(235.90)

$R_1$  found from run to run under similar experimental conditions. The extracted values of  $R_1$  and  $P_1/P_0$  also depend on the Ps energy distribution which is related to the Ps work function. The ratio,  $R_1$ , is obtained by using the values of  $T_1$  and  $P_1$  measured by extrapolation to low-incident positron energies at the highest sample temperatures. The values deduced for  $R_1$  in these samples are within 10% of those which we obtained for a hot Ge target ( $\sim 900^\circ\text{C}$ ). Mills<sup>2</sup> showed that the corresponding  $\gamma$ -ray spectrum of hot Ge was consistent with the Ps fraction of 100% using a Ge(Li) detector. The values obtained for  $R_1$ ,  $R_0$ , and  $P_1/P_0$  depend on not only the  $\gamma$ -ray energy region but also on the characteristics of the detector. The corresponding ratios computed with the valley are  $R_{S0}$  and  $R_{S1}$  for 0% and 100% Ps, respectively. The limiting values for these ratios are obtained by the same method as  $R_1$  and  $R_0$  (see Table I). Using a  $^{68}\text{Ge}$  positron emitting source sealed between two pieces of Al and inserted in place of the sample, the 0% Ps limit was checked. In this experiment we found significant variations in  $R_0$  associated with count rate and some variation attributable to scattering of the annihilation photons from the sample.

Agreement to within approximately 10% was found, when the background was subtracted.

The above method has the inherent error that if any of the  $^3\text{S}_1$  Ps atoms suffer wall collisions and undergo a pickoff process they will decay by two photons. The size of this factor will be dependent on the energy and spatial distribution of the emitted Ps. In our experiment we have tried to minimize this effect by placing the target in an open region. Some of the positrons may find a deep trap on the surface and may not be detrapped at a rate much faster than the annihilation rate at the surface, thus also affecting  $R_1$ .

The numerical estimates of these peak values and those for the valley region are listed in Table I. Slightly different energy window widths on the SCA's were used for different samples, and therefore relative comparisons of these extracted values between samples are not to be greatly trusted. The valley to total ratios are used as a self-consistent check of the data. Some variation between peak and valley to total ratios was found. Data obtained in this manner for the positronium fraction, as a function of temperature and incident positron energy, are shown in Figs. 1-3.

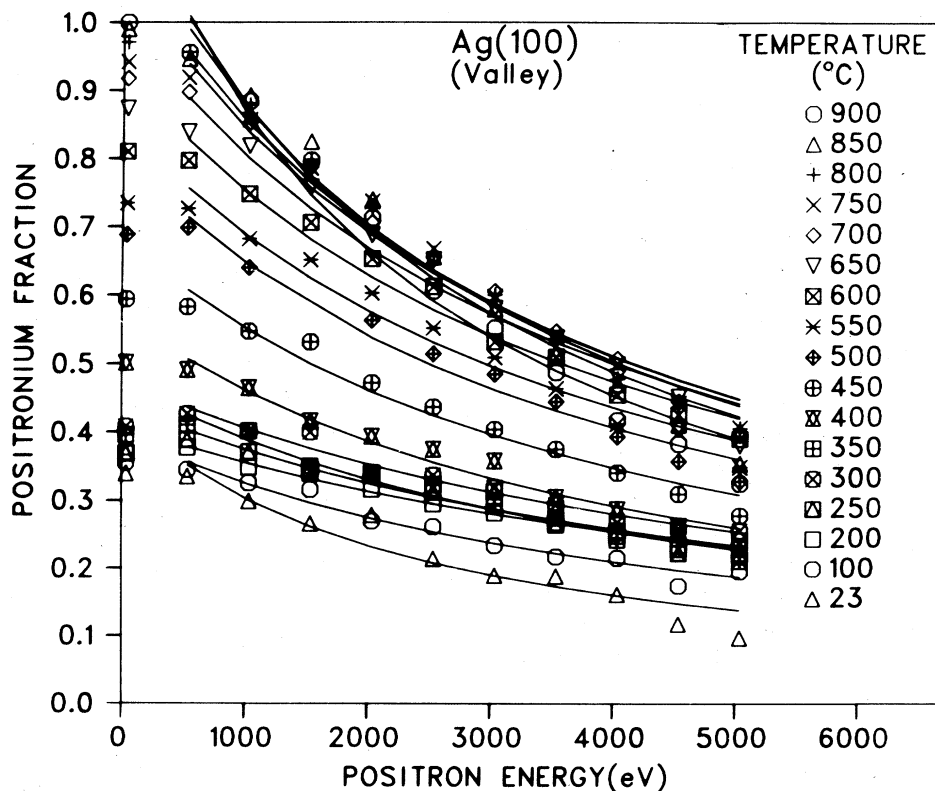


FIG. 1. Positronium fraction as calculated by Eq. (2) for Ag(100) is shown as a function of incident positron energy. The solid lines are the best fit lines of Eq. (5) through the data, where  $T_r = 1$ . Auger spectra showed  $< 1\%$  C, O, and approximately 1% P after runs for both Ag(100) and Ag(111). A sharp LEED pattern was observed for Ag(100). The peak or valley to total ratios used in calculating the positronium fraction are listed in Table I as peak or valley, respectively.

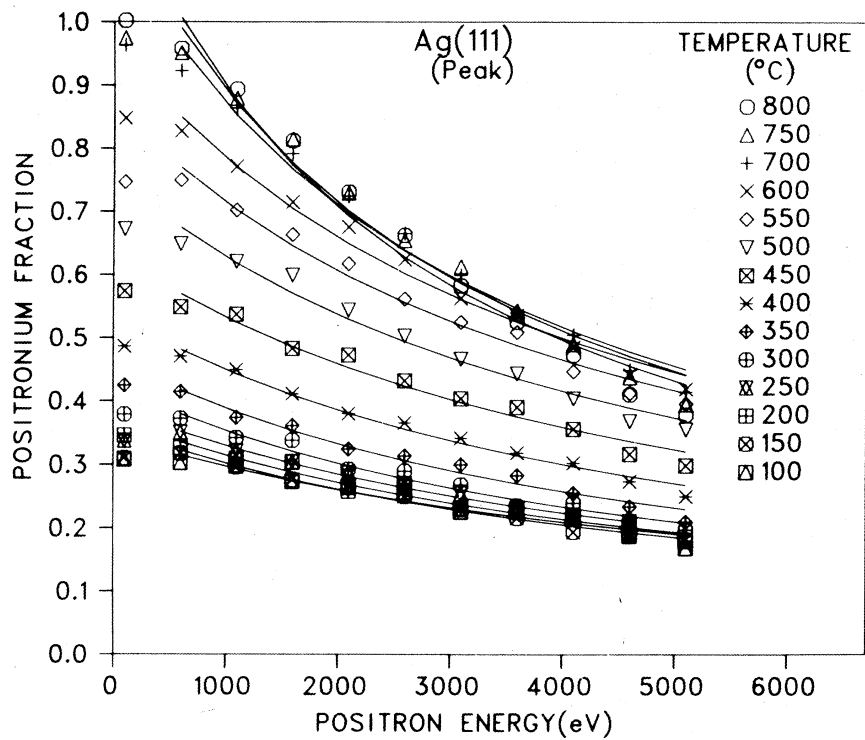


FIG. 2. Positronium fraction for Ag(111) is shown as a function of the incident positron energy for different sample temperatures. Sharp LEED spots were observed before and after the run.

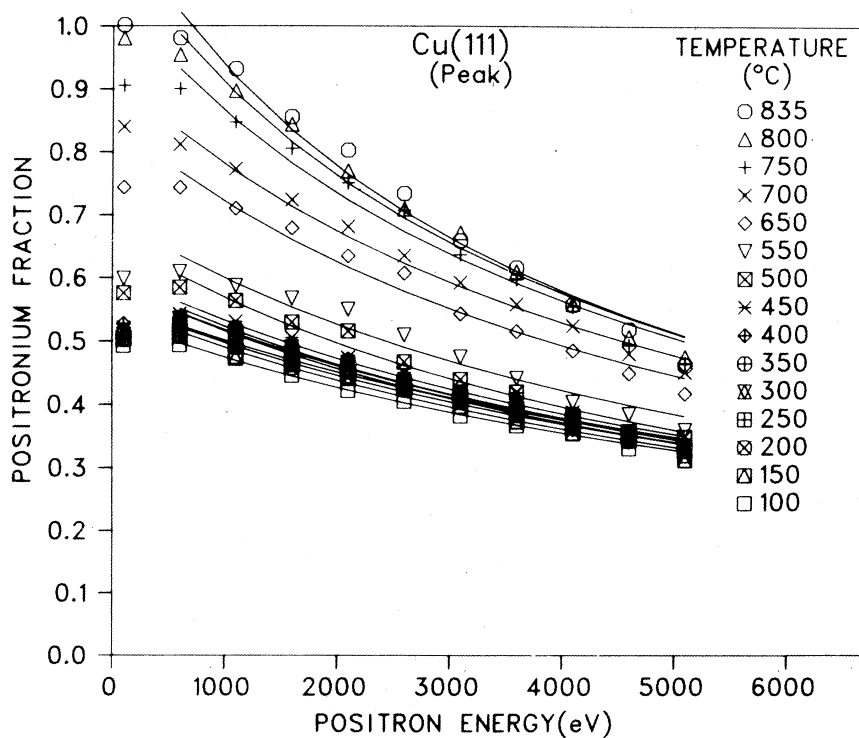


FIG. 3. Positronium fraction for Cu(111) as a function of the incident positron energy at different sample temperatures. Approximately 10% S and 1.0% P was brought to the surface after the high-temperature run.

#### IV. THEORY AND ANALYSIS OF RESULTS

Our method of interpreting the data is based on the following physical picture. The incident positron quickly thermalizes ( $<10^{-12}$  sec) and subsequently diffuses through the lattice until either: (i) it is annihilated in the lattice (i.e., "annihilation in the bulk"), (ii) it is trapped by a lattice vacancy and is eventually annihilated there, or (iii) it reaches the surface where it is trapped,<sup>3,7,8</sup> reflected back into the lattice or emitted into the vacuum. If the positron is trapped at the surface, it either annihilates there or is reemitted into the vacuum as positronium.

In connection with a similar experimental study, Mills<sup>2</sup> presented a formula for the dependence of the Ps fraction upon incident positron energy based on the solution of the one-dimensional diffusion equation in a semi-infinite crystal with a perfectly absorbing surface which includes annihilation in the bulk. We present in Appendix A an explicit derivation of a formula for the incident-energy dependence based on assumptions similar to, but less restrictive than, those employed by Mills, and, as did Mills, we describe the positron motion after thermalization by the diffusion equation.<sup>17</sup> In this derivation we account for the presence of trapping centers such as vacancies by replacing the annihilation rate  $\tau^{-1}$  with an effective annihilation rate

$$\tau_{\text{eff}}^{-1} \equiv \tau^{-1} + \sum_{i=1}^N K_i, \quad (3)$$

where  $K_i$  is the probability per second that a freely diffusing positron is trapped at a defect of species  $i$ . We assume that, once trapped in a vacancy, positrons have a negligible probability of reemission from the trapping center, and we assume that positrons which are in a layer of thickness  $\lambda$  at the surface can be removed from the crystal by emission into the vacuum as positronium or free positrons, and by trapping and annihilation at the surface. The boundary condition at the surface will be determined by competition between the rate of these removal events and the rate of scattering and reflection back into the crystal; we describe this competition by use of the so-called "radiative boundary condition."<sup>18</sup>

In the derivation described in the Appendix we have used a simple exponential form for the initial probability distribution of the implanted positron<sup>19</sup>

$$C_0(x) = \alpha e^{-\alpha x/S}, \quad (4)$$

where  $S$  is the surface area of the crystal and  $\alpha^{-1}$  is the mean depth of implantation. Following Mills,<sup>2</sup> we assume the latter depends linearly on the implantation energy  $E$ ; i.e.,  $\alpha^{-1} = E/A$ . Recently Mills and Murray<sup>20</sup> have discussed the use of more general implantation profiles, and in a later paper<sup>21</sup> we will discuss the effect of different initial distributions.

With the assumptions described above, and on the assumption that monovacancies in thermal equilibrium are the only trapping centers present in appreciable numbers, we find that the positronium fraction  $F$  is given by

$$F = T_r F_0 / \left( \frac{E}{E_0} + 1 \right), \quad (5)$$

where  $F_0$  is the branching ratio for positronium formation of the positrons removed through the surface at  $E=0$  and

$$E_0 \equiv A (D \tau_{\text{eff}})^{1/2} = \frac{A (D \tau)^{1/2}}{[1 + \tau \mu \exp(S_{1v}^f/k) \exp(-E_{1v}^f/kT)]^{1/2}} \quad (6)$$

$\mu$ ,  $S_{1v}^f$ , and  $E_{1v}^f$  are the monovacancy specific trapping rate, formation entropy, and enthalpy, respectively.  $T_r$  is a transmission coefficient for the surface which varies from zero to unity and is given by

$$T_r \equiv \frac{(\lambda/\langle l \rangle) [(\Gamma_r \tau_s)(\Gamma_r \tau_{\text{eff}})]^{1/2}}{1 + (\lambda/\langle l \rangle) [(\Gamma_r \tau_s)(\Gamma_r \tau_{\text{eff}})]^{1/2}} \quad (7)$$

This depends upon the values of the surface removal rate  $\Gamma_r$ , compared with the positron scattering rate,  $\tau_s^{-1}$ , and the annihilation rate in the interior,  $\tau_{\text{eff}}^{-1}$  [see Eq. (3)], and on the relative value of the thickness of the surface region,  $\lambda$ , compared with the positron mean free path  $\langle l \rangle$ .

The dependence upon incident positron energy,  $E$ , of the fraction,  $F$ , of positrons reemitted as positronium from Ag(100), Ag(111), and Cu(111) surfaces is described quite well by Eq. (5) for energies in the range  $500 \leq E \leq 5000$  eV, as may be seen from Figs. 1-3.  $E_0(T)$  is a free parameter here and the values obtained are shown in Figs. 4-6.

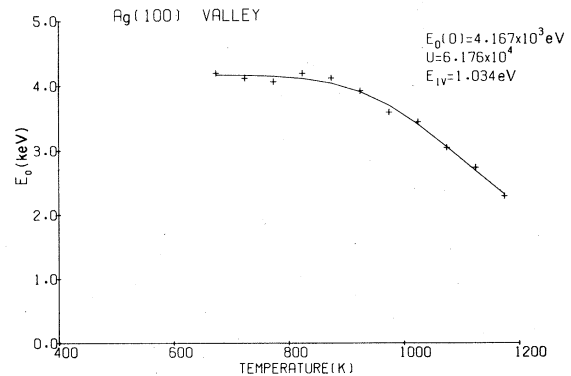


FIG. 4. Temperature dependence of  $E_0$  for Ag(100). The solid line represents the best fit of Eq. (6) through the data points. The fitting parameter  $U$  is equal to  $\tau \mu \exp(S_{1v}^f/k)$ , where  $E_0(0)$  is the low-temperature value of  $E_0$ .

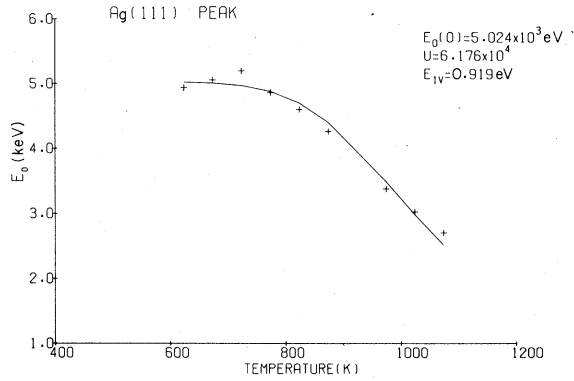


FIG. 5. Temperature dependence of  $E_0$  for Ag(111). The solid line represents the best fit of Eq. (6) through the data points.

The temperature dependence of the effective lifetime of free positrons,  $\tau_{\text{eff}}$ , as manifested in the parameter  $E_0$  is quite adequately described by Eq. (6), as may be seen in Figs. 4–6. The values obtained for  $E_{1v}^f$  of Ag are 1.03 and 0.9 eV from the (100) and (111) surfaces, respectively. These variations in  $E_{1v}^f$  most likely provide an estimate of the systematic errors involved in these measurements. These values are about 10–20% lower than the currently accepted bulk value, 1.13 eV.<sup>22</sup> A value of  $0.9 \pm 0.2$  eV was obtained from the Cu(111) data, about 30% lower than the bulk value, 1.27 eV, for  $E_{1v}^f$  in Cu.<sup>23</sup> Calibration errors in  $R_0$  can affect these deduced values.

Further discussion of the temperature dependence of the positronium fraction requires explicit consideration of the branching ratio for positronium formation,  $F_0$ , which appears in Eq. (5). In the development of the equation we assume that a positron diffusing to the surface may be removed from the interior into the vacuum through the surface, in general, as either a free positron or as positronium,

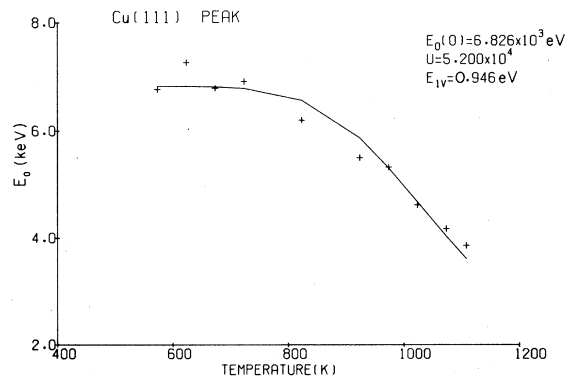


FIG. 6. Temperature dependence of  $E_0$  for Cu(111). The solid line is the best fit of Eq. (6) through the data points.

or it may be removed from the interior into the surface by trapping. Once trapped at the surface, a positron may be emitted from the trap by thermal activation subsequently forming Ps or may be annihilated while still in the surface trap. The branching ratio is obtained from the relative probabilities of these processes. The emission rate from the interior into the vacuum is denoted by  $\Gamma_{em}$  and the rate of trapping by the surface as  $\Gamma_t$ . Of the emitted positrons, we assume that a fraction  $m$  are emitted as positronium. For a positive positron work function,  $\Phi_p$  (unfavorable for reemission into the vacuum)  $m$  is expected to be near unity. Furthermore denote the rate at which trapped positrons are emitted into the vacuum by  $\Gamma_{em,t}$ , of which a fraction,  $m_t$ , are emitted as positronium. Finally,  $\tau_t^{-1}$  is the rate of annihilation of positrons trapped at the surface. These rates can be combined in a straightforward manner to yield for the branching ratio

$$F_0 = \frac{m\Gamma_{em}}{\Gamma_{em} + \Gamma_t} + \frac{\Gamma_t}{\Gamma_{em} + \Gamma_t} \left( \frac{\Gamma_{em,t}m_t}{\Gamma_{em,t} + \tau_t^{-1}} \right) \quad (8)$$

The first term on the right-hand side is the probability of emission as positronium directly from the interior without being trapped prior to emission; the second term is the probability of positronium formation by thermally activated emission from the trapped state.

If we further assume that the only significantly temperature dependent process of those discussed above is thermally activated emission from the surface trap and describe the temperature dependence as:

$$\Gamma_{em,t} = \nu \exp(-\Delta E/kT) \quad (9)$$

then the temperature dependence of the branching ratio,  $F_0$ , becomes

$$F_0 = \frac{C_1[1 + C_2 \exp(-\Delta E/kT)]}{[1 + C_3 \exp(-\Delta E/kT)]} \quad (10)$$

where

$$C_1 \equiv m\Gamma_{em}/(\Gamma_{em} + \Gamma_t) \quad (11a)$$

$$C_2 \equiv \nu\tau_t(1 + m_t\Gamma_t/m\Gamma_{em}) \quad (11b)$$

and

$$C_3 \equiv \nu\tau_t \quad (11c)$$

Note that the combination of these constants

$$\frac{C_1 C_2}{C_3} = \frac{\Gamma_{em} + m_t\Gamma_t}{\Gamma_{em} + \Gamma_t} \quad (12)$$

should be less than or equal to unity since, by their definition,  $m$  and  $m_t$  are less than or equal to unity. In this simple analysis  $\nu$ , a frequency factor, is assumed to be temperature independent.

The data shown in Figs. 1–3 were used to extract

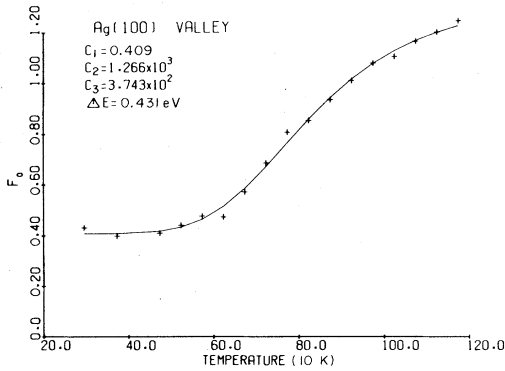


FIG. 7. Values of  $F_0$ , obtained by fitting the positronium fraction data to Eq. (5), are shown as a function of temperature for Ag(100). The solid line is the best fit of Eq. (10) through the data. The parameters shown in the figure are described by Eqs. (10)–(11c).

values of  $T_r F_0$  using Eq. (5). The transmission coefficient,  $T_r$ , was assumed to be unity (or strictly speaking, assumed to be approximately temperature independent) and the temperature dependence of the resulting values of  $F_0$  were fitted by Eq. (10). The results are shown in Figs. 7–9, and the fit to the data provided by Eq. (10) is seen to be quite good. The activation energy associated with the thermal emission process was found to be  $0.43 \pm 0.1$ ,  $0.46 \pm 0.1$ , and  $0.52 (+0.2, -0.1)$  eV for Ag(100), Ag(111), and Cu(111) surfaces, respectively.

A slightly different way of analyzing the data yields essentially the same values of the activation energy. This is illustrated by the behavior of the Ag(100) data. In the method described above, isothermal data as a function of energy in the range  $50 \leq E \leq 5000$  eV were analyzed to obtain one value of  $F_0$  for each temperature, and the results were fitted with Eq. (10) to yield a value of  $\Delta E$ . Consider now data at constant

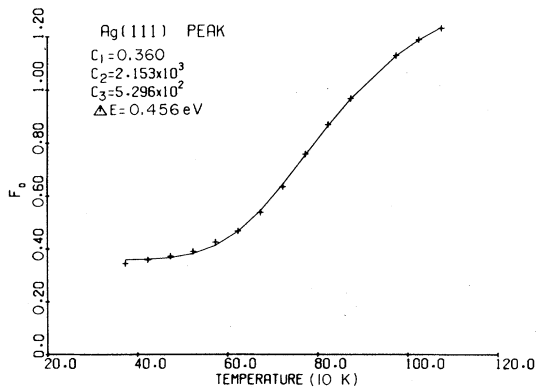


FIG. 8. Temperature dependence of  $F_0$  for Ag(111). The best fit of Eq. (10) is shown as a solid line.

incident positron energy analyzed as a function of  $T$ . Such data are shown in Fig. 10. For temperatures low enough that insufficient vacancies are present to cause a significant variation of  $E_0$  with temperature, the temperature dependence of  $F$  should be dominated by the activated emission process; based on this assumption the temperature dependence of  $F$  should be reasonably well described by Eq. (10) with  $F_0$  replaced by  $F$ . The solid curves of Fig. 10 were obtained in this manner, and it can be seen that the data for  $T \leq 1023$  K are described quite well by this means. Each curve obtained at a particular value of the incident positron energy  $E$  yields a value of  $\Delta E$ ; these values are shown as a function of  $E$  in Fig. 11. The values approach 0.45 eV for  $E$  less than about 1000 eV in good agreement with a value of 0.43 eV obtained by fitting the isothermal curves with Eq. (10). These variations in  $\Delta E$  are thought to be associated with thermal vacancies, with the effect on the extracted activation energies more serious at the higher incident positron energies.

The physical interpretation of the activation energy  $\Delta E$  is made uncertain due to a lack of knowledge of the mechanism by which positrons are emitted. Mills has used an interpretation based on a Born-Haber cycle to estimate the binding energy of the surface trap for positrons for such data.<sup>7</sup> The energy required to remove the positrons from a surface trap to rest at infinity is the binding energy,  $E_{ST}$ . The energy required to remove an electron from the metal to rest at infinity is the electron work function  $\Phi_e$ . Upon combining the two to form positronium the binding energy, 6.8 eV, is released. Thus the energy required to form positronium at rest far from the metal surface is  $E_{ST} + \Phi_e - 6.8$  eV. This picture ignores interaction with any surface electron states. Mills identifies this with the activation energy for thermal emission of positronium.<sup>7</sup> However, this must be a lower limit since it may well be necessary to excite the trapped positron to a larger energy providing a dis-

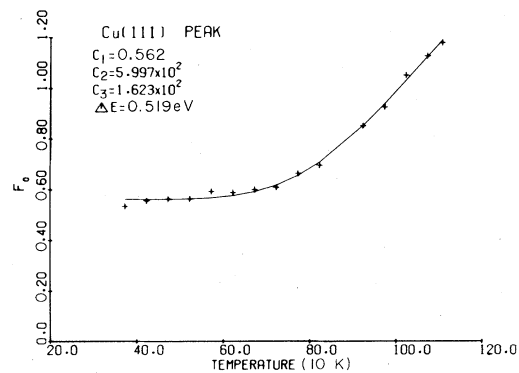


FIG. 9. Temperature dependence of  $F_0$  for Cu(111). These fitted values are known to be sensitive to S impurities.



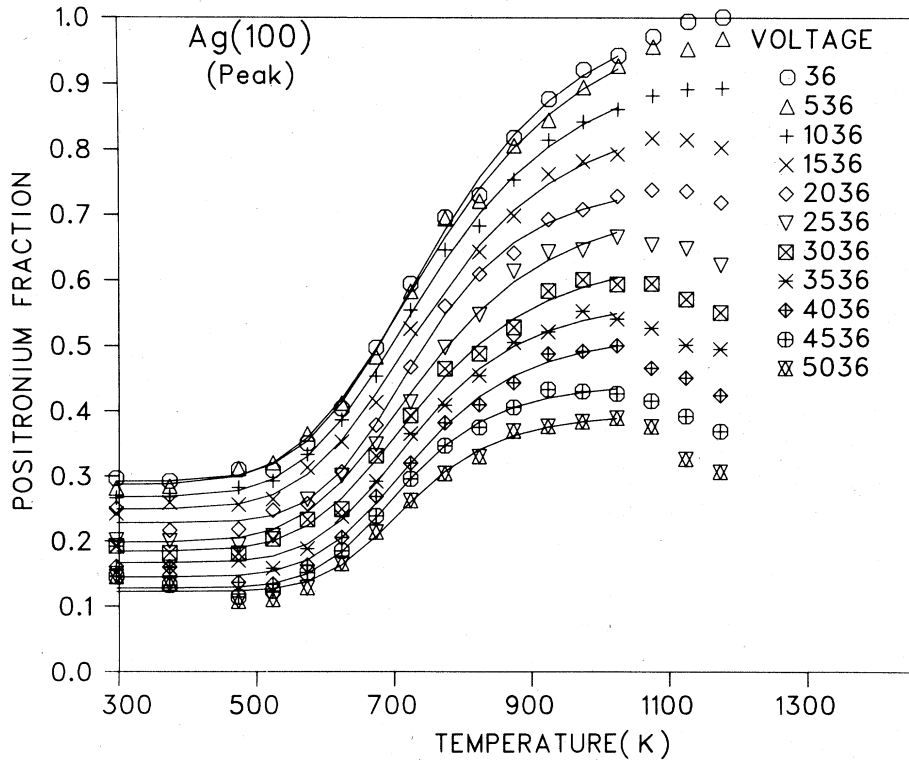


FIG. 10. Fraction of positrons converted to positronium ( $F$ ) vs temperature at different incident positron energies for Ag(100). The fitted curves to Eq. (10) are shown as solid lines and include data points to 1023 K. The negative curvature in the data at the higher sample temperatures and voltages is associated with positron trapping at vacancies.

tance far enough from the surface that the electron density is sufficiently low<sup>4</sup> that positronium can form. This is illustrated schematically in Fig. 12 where  $\Phi_p$  is shown to be a positive positron work function (unfavorable for reemission into the vacuum).<sup>23</sup> The first mention of a positron surface trap was by Ma-

dansky and Rasetti<sup>24</sup> which was later theoretically formulated by Hodges and Stott<sup>25</sup> to explain the lack of positronium formation found in voids in neutron irradiated metals. Thus, we can say, based on the Born-Haber cycle that the surface trap depth is less than a certain value

$$E_{ST} \leq \Delta E + 6.8 \text{ eV} - \Phi_e$$

The values of  $\Delta E$  deduced from the data of Figs. 7-9 together with electron work function values of 4.81, 4.75, and 4.85 eV (Ref. 26) yield maximum trap

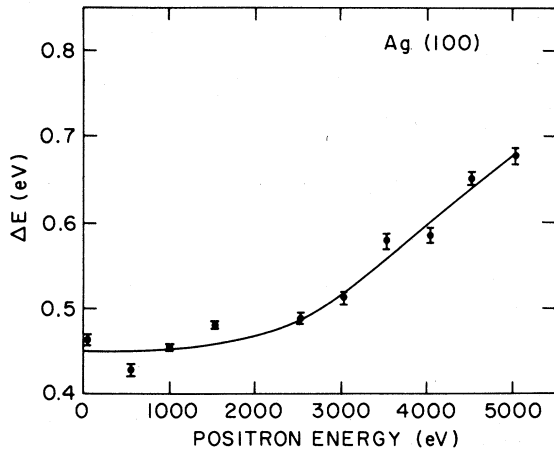


FIG. 11. Values of an effective  $\Delta E$  [Eq. (10)] are shown as a function of incident positron energy for Ag(100). The values of  $\Delta E$  were obtained from the fits shown in Fig. 10. The solid line is shown as a guide.

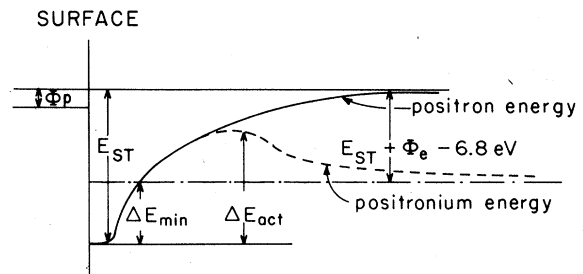


FIG. 12. Relationship between the activation energy for positronium emission,  $\Delta E_{min}$ , and the actual activation energy,  $\Delta E_{act}$ , is based on the Born-Haber cycle, and  $\Phi_p$ ,  $\Phi_e$  are the positron and electron work functions, respectively.

depths of  $2.42 \pm 0.1$ ,  $2.49 \pm 0.1$ , and  $2.38 (+0.2, -0.1)$  eV for Ag(100), Ag(111), and Cu(111) surfaces, respectively.

## V. CONCLUSIONS

We have shown on clean surfaces of Cu and Ag that the measured positronium fraction is temperature and incident-energy dependent. A general one-dimensional diffusion model has been presented and compared to the data for both positive and negative positron work function metals. A good agreement between the theory and the data is obtained with the simple model. The presence of internal traps has been included in the diffusion model by using an effective annihilation time. By employing this model we find that vacancy formation energies can be extracted from the data. The formation energies obtained from the fits to the data are below the accepted bulk vacancy formation energies.

The positronium fraction has been found to be strongly temperature dependent in both positive and negative positron work function metals. This temperature dependence is identified with thermally activated emission from a surface trap. The model presented describes the data well and an activation energy associated with this thermal emission process was extracted from the data. A lower limit is deduced for the depth of this surface trap by utilizing a Born-Haber cycle. The exact process or branching ratio of positronium emission from clean metal surfaces still remains uncertain and is presently under investigation. A detailed understanding of the positronium yield and the possible implications for slow positron emission, low-energy positron reflection, and the positron work function await further experimental and theoretical developments.

## ACKNOWLEDGMENTS

The authors wish to thank E. Bonderup, D. Jepsen, A. Goland, A. Mills, and I. K. MacKenzie for useful comments. Appreciation is also extended to M. McKeown for computer work and M. Carroll and J. Hurst for technical support. This research was supported by the Division of Basic Energy Sciences of the U. S. DOE.

## APPENDIX: THE POSITRONIUM FRACTION PRODUCED BY A TRAP-CONTAINING CRYSTAL WITH A PARTIALLY REFLECTING BOUNDARY

In connection with a similar experimental study, Mills<sup>2</sup> presented a formula for the dependence of the

Ps fraction upon incident positron energy based on the solution of the one-dimensional diffusion equation in a semi-infinite crystal with a perfectly absorbing surface and which includes annihilation in the bulk. We present here an explicit derivation of a formula for the incident-energy dependence based on assumptions similar to, but less restrictive than, those employed by Mills,<sup>2</sup> and, as did Mills, we describe the positron motion after thermalization by the diffusion equation.<sup>17</sup>

If  $W(\vec{r}', t; \vec{r}) d\vec{r}'$  is the probability that a positron, at  $\vec{r}$  when  $t=0$ , will have diffused into the volume  $d\vec{r}'$  at  $\vec{r}'$  after a time  $t$  and  $C_0(\vec{r})$  is the initial probability density for the positron, then the probability density evolves with time as

$$C(\vec{r}', t) = \int C_0(\vec{r}) W(\vec{r}', t; \vec{r}) d\vec{r} \quad (\text{A1})$$

By Fick's law, the flux of probability at the point  $\vec{r}'$  at time  $t$  is

$$\begin{aligned} J(\vec{r}', t) &= -D \nabla C(\vec{r}', t) \\ &= -D \int C_0(\vec{r}) \nabla W(\vec{r}', t; \vec{r}) d\vec{r} \quad (\text{A2}) \end{aligned}$$

where the gradient under the integral is taken with respect to the variable  $\vec{r}'$ , and  $D$  is the positron diffusion coefficient. The probability function  $W$  is the fundamental solution of the diffusion equation starting with a  $\delta$  function, modified to include the disappearance of positrons by annihilation

$$\frac{\partial W}{\partial t} = D \nabla^2 W - \tau^{-1} W \quad (\text{A3})$$

where  $\tau^{-1}$  is the probability per second that a freely diffusing positron will be annihilated. The form of the fundamental solution  $W$  depends upon the boundary conditions. There are two factors which determine the boundary conditions in this problem: the existence of the free surface and the existence of trapping centers, such as vacancies, in the crystal interior. We shall account for the latter effect approximately by using an effective annihilation rate, rather than, more correctly, through the boundary conditions. That is, we account for the presence of internal traps by replacing the annihilation rate,  $\tau^{-1}$ , by an effective annihilation rate

$$\tau_{\text{eff}}^{-1} = \tau^{-1} + \sum_{i=1}^N K_i \quad (\text{A4})$$

where  $K_i$  is the probability per second that a freely diffusing positron is trapped at a trap of species  $i$ . The use of an effective annihilation rate should be a good approximation for trapping if the intertrap spacing is small compared with the scale of the spatial variation of the initial positron probability distribution and for times large compared with an initial transient of duration  $\sim r_0^2/D$ , where  $r_0$  is the capture radius of the trap.<sup>18</sup> Furthermore, we assume that, once

trapped, positrons have a negligible probability of reemission out of the vacancy. No detrapping out of vacancies has been observed in bulk positron measurements for either Ag or Cu.

Consider now the effect of the free surface on the boundary condition for Eq. (A3). We shall assume that positrons which are in a layer of thickness  $\lambda$  at the surface can be removed from the crystal by emission into vacuum as positronium or free positrons, and by trapping and annihilation at the surface. Let the total rate of these "removal" processes be denoted by  $\Gamma_r$ . The boundary condition at the surface will be determined by a competition between the removal rates of these processes and the rate of scattering and reflection back into the crystal. Problems of a similar nature arise in radiative heat transfer,<sup>27</sup> chemical kinetics,<sup>18</sup> and loss of moisture from media by surface evaporation.<sup>28</sup> In such cases, an approximate

solution has been obtained by adjusting the boundary condition so that the rate of removal from the surface just balances the rate of supply by the diffusive flux; in our case such a "radiative" boundary condition<sup>18</sup> becomes (for a surface at  $x=0$ )

$$\lambda C(0,t)\Gamma_r = |J(0,t)| \quad (A5)$$

With Eqs. (A1) and (A2) and the assumption that the initial probability density  $C_0(x)$  is a function only of  $x$ , as is the case in these experiments, one obtains the radiative boundary condition

$$\frac{\lambda\Gamma_r}{D} = \int_0^\infty C_0(x) \frac{\partial W}{\partial x'} \Big|_{x'=0} dx / \int_0^\infty C_0(x) W(0,t;x) dx \quad (A6)$$

A form for  $W$  which satisfies Eq. (A3) with  $\tau$  replaced by  $\tau_{\text{eff}}$  is

$$W(x',t;x) = \frac{1}{2(\pi Dt)^{1/2}} \left[ \exp\left(-\frac{(x-x')^2}{4Dt}\right) + Q \exp\left(-\frac{(x+x')^2}{4Dt}\right) \right] \exp\left(\frac{-t}{\tau_{\text{eff}}}\right) \quad (A7)$$

The "boundary condition parameter"  $Q$  varies with time so as to satisfy Eq. (A6). When  $Q=+1$ ,  $W$  is correct for a perfectly reflecting boundary,<sup>29</sup> i.e., when  $\lambda\Gamma_r/D \rightarrow 0$ , while for  $Q=-1$ ,  $W$  corresponds to a perfectly absorbing boundary,<sup>29</sup> i.e., when  $\lambda\Gamma_r/D \rightarrow \infty$ .

This approach yields a formal solution which can numerically be evaluated for any initial probability density  $C_0(x)$ . At any chosen time  $W(x',t;x)$  as given by Eq. (A7) is inserted in Eq. (A6), and after evaluation of the integrals, the resulting equation is solved for  $Q$ , which is then inserted in Eq. (A7) to yield  $W(x',t;x)$  appropriate to that time. The number of positrons being removed from the surface layer per sec per unit area at that time is given by

$$N(t) = \lambda\Gamma_r \int_0^\infty C_0(x) W(0,t;x) dx \quad (A8)$$

This process is then repeated for each desired value of the time.

An approximate derivation of a closed-form solution to this problem, which becomes exact in the limit of a perfectly absorbing or perfectly reflecting surface, can be obtained as follows. First an explicit expression for the initial positron distribution is required; this we take to be given by<sup>19</sup>

$$C_0(x) = \alpha e^{-\alpha x/S} \quad (A9)$$

where  $\alpha^{-1}$  is the mean depth of implantation and  $S$  is the surface area of the crystal. A derivation with different initial distributions will be presented in a later paper.<sup>21</sup> With this form of  $C_0(x)$ , Eqs. (A6) and (A7) yield for the boundary condition parameter

$$Q(t) = \frac{1 - z(t)(1 + \lambda\Gamma_r/\alpha D)}{1 - z(t)(1 - \lambda\Gamma_r/\alpha D)} \quad (A10a)$$

where

$$z(t) = \sqrt{\pi} \alpha (Dt)^{1/2} \exp(\alpha^2 Dt) \operatorname{erfc}[\alpha (Dt)^{1/2}] \quad (A10b)$$

$z$  depends on time through the dimensionless variable  $\alpha(Dt)^{1/2}$  and ranges between zero and unity. We obtain the desired approximate solution by using an average value for  $z$  in Eq. (A10a) to obtain a time-independent boundary condition parameter  $Q$ . We have chosen to average  $z$  by a weighted integral average over the dimensionless variable  $\alpha(Dt)^{1/2}$ , with a plausible weighting factor being the probability decay factor  $\exp(-t/\tau_{\text{eff}})$

$$\begin{aligned} \langle z \rangle &= \frac{\int_0^\infty \exp(-t/\tau_{\text{eff}}) z [\alpha(Dt)^{1/2}] d[\alpha(Dt)^{1/2}]}{\int_0^\infty \exp(-t/\tau_{\text{eff}}) d[\alpha(Dt)^{1/2}]} \\ &= \frac{\alpha(D\tau_{\text{eff}})^{1/2}}{1 + \alpha(D\tau_{\text{eff}})^{1/2}} \quad (A11) \end{aligned}$$

Thus  $\langle z \rangle$  depends upon the relative values of the mean implant depth  $\alpha^{-1}$ , and the mean diffusion length,  $(D\tau_{\text{eff}})^{1/2}$ . The only justification for using this approximation is that it yields the exact solution for the surface behaving as a perfect absorber or as a perfect reflector of positrons. Thus we expect the approximation to be reasonably good for intermediate cases. Recent work by Mills and Murray<sup>20</sup> and by Jorch *et al.*<sup>21</sup> has shown that the positronium fraction obtained by this approximation is, in fact, exact.

Combining Eqs. (A7)–(A11) yields the probability per second per unit area  $N(t)$  [Eq. (A8)] that the implanted positron is removed from the crystal at the

surface by either emission or annihilation (rather than by annihilation in the crystal interior); integrating  $N(t)$  over all time and multiplying by the surface area of the crystal yields the probability  $P$  that the positron is removed through the crystal surface rather than annihilating in the crystal interior

$$P = \left( \frac{(\lambda/\langle l \rangle)[(\Gamma_r \tau_s)(\Gamma_r \tau_{\text{eff}})]^{1/2}}{1 + (\lambda/\langle l \rangle)[(\Gamma_r \tau_s)(\Gamma_r \tau_{\text{eff}})]^{1/2}} \right) \frac{\alpha(D\tau_{\text{eff}})^{1/2}}{1 + \alpha(D\tau_{\text{eff}})^{1/2}}$$

$$\equiv T_r \frac{\alpha(D\tau_{\text{eff}})^{1/2}}{1 + \alpha(D\tau_{\text{eff}})^{1/2}}, \quad (\text{A12})$$

where in the first term (in large parentheses) the positron diffusion coefficient was replaced by  $\langle r \rangle^2/\tau_s$ , where  $\langle l \rangle$  is the positron mean free path

and  $\tau_s$  is the mean time between scatterings. The factor  $T_r$  is a "transmission coefficient" for the partially reflecting boundary. The positronium fraction,  $F$ , is obtained by multiplying the probability  $P$  by the branching ratio,  $F_0$ , for positronium formation of the positrons which are removed through the surface:

$$F = PF_0 = \frac{T_r F_0 \alpha(D\tau_{\text{eff}})^{1/2}}{[1 + \alpha(D\tau_{\text{eff}})^{1/2}]} \quad (\text{A13})$$

If  $\tau_{\text{eff}}$  is obtained from Eq. (A4) by assuming that the only trapping centers present in appreciable numbers are monovacancies present in thermal equilibrium and if it is assumed<sup>2</sup> that the mean implant depth  $\alpha^{-1}$  varies linearly with the energy  $E$  of the incident positron,  $\alpha^{-1} = E/A$ , then one obtains the expressions for the positron fraction given in Sec. IV Eqs. (5)–(7).

<sup>1</sup>K. F. Canter, A. P. Mills, Jr., and S. Berko, *Phys. Rev. Lett.* **33**, 7 (1974).

<sup>2</sup>A. P. Mills, Jr., *Phys. Rev. Lett.* **41**, 1828 (1978).

<sup>3</sup>K. G. Lynn, *J. Phys. C* **12**, L435 (1979); *Phys. Rev. Lett.* **43**, 391, 803(E) (1979).

<sup>4</sup>A. Held and S. Kahana, *Can. J. Phys.* **42**, 1908 (1964); D. N. Lowy and A. D. Jackson, *Phys. Rev. B* **12**, 1689 (1975).

<sup>5</sup>O. Mogensen, K. Petersen, R. M. J. Cotterill, and B. Hudson, *Nature* **239**, 98 (1972); R. M. J. Cotterill, I. K. MacKenzie, L. Smedskjaer, G. Trumpy, and J. H. O. L. Träff, *ibid.* **239**, 99 (1972).

<sup>6</sup>A preliminary account of this work was presented at the 5th International Conference on Positron Annihilation, Mt. Fuji, Japan (1979) (unpublished).

<sup>7</sup>A. P. Mills, Jr., *Solid State Commun.* **31**, 623 (1979).

<sup>8</sup>C. H. Hodges and M. J. Stott, *Solid State Commun.* **12**, 1153 (1973).

<sup>9</sup>A. P. Mills, Jr., *Appl. Phys. Lett.* **36**, 427 (1979).

<sup>10</sup>K. F. Canter, P. G. Coleman, T. C. Griffith, and G. R. Heyland, *J. Phys. B* **5**, L167 (1972); K. G. Lynn and B. T. A. McKee, *Appl. Phys.* **19**, 247 (1979).

<sup>11</sup>K. G. Lynn and H. Lutz, *Rev. Sci. Instrum.* (to be published).

<sup>12</sup>K. G. Lynn (unpublished).

<sup>13</sup>A. Ore and J. L. Powell, *Phys. Rev.* **75**, 1696 (1949).

<sup>14</sup>M. Leventhal, *Ap. J.* **183**, L147 (1973).

<sup>15</sup>P. Schultz and K. G. Lynn (unpublished data).

<sup>16</sup>S. Marder, V. W. Hughes, C. S. Wu, and W. Bennett, *Phys. Rev.* **103**, 1258 (1956).

<sup>17</sup>This approximation to the more appropriate Boltzmann equation for positron transport should be adequate for

positrons implanted at distances from the surface much greater than the mean free path between scattering events. A discussion of the adequacy of the diffusion approximation to the Boltzmann equation is found in Chap. 8 of K. M. Case and P. F. Zweifel, *Linear Transport Theory* (Addison-Wesley, Reading, Mass., 1967).

<sup>18</sup>T. R. Waite, *Phys. Rev.* **107**, 463 (1957).

<sup>19</sup>W. Brandt, *Appl. Phys.* **5**, 1 (1976).

<sup>20</sup>A. P. Mills, Jr. and C. A. Murray, *Appl. Phys.* (to be published).

<sup>21</sup>H. Jorch, K. G. Lynn, and D. O. Welch (unpublished).

<sup>22</sup>J. L. Campbell, C. W. Schulte, and R. P. Gingerich, *J. Nucl. Mater.* **69** and **70**, 609 (1978).

<sup>23</sup>W. Trifh user and J. D. McGervey, *Appl. Phys.* **6**, 177 (1975).

<sup>24</sup>L. Madansky and F. Rasetti, *Phys. Rev.* **79**, 397 (1950).

<sup>25</sup>C. H. Hodges and M. J. Stott, *Phys. Rev. B* **7**, 73 (1973); R. M. Nieminen and C. H. Hodges, *Solid State Commun.* **18**, 1115 (1976).

<sup>26</sup>The Ag(100) and Ag(111) work functions were obtained from *Chemistry and Physics*, 49th ed. (Chemical Rubber, Cleveland, 1975); and the Cu(111) work function from P. O. Gartland and B. J. Slagsvold, *Phys. Rev. B* **12**, 4047 (1975).

<sup>27</sup>H. S. Carslaw and J. C. Jaeger, *Conduction of Heat in Solids* (Clarendon, Oxford, 1947).

<sup>28</sup>J. Crank, *The Mathematics of Diffusion* (Clarendon, Oxford, 1956).

<sup>29</sup>J. R. Manning, *Diffusion Kinetics for Atoms in Crystals* (Van Nostrand, Princeton, 1968).